CENTER FOR
TRANSPORTATION STUDIES

UNIVERSITY OF MINNESOTA

RESEARCH REPORT

Superbus Phase I: Accessory Loads Onboard a Parallel Hybrid-Electric City Bus

Jeffrey S. Campbell
David B. Kittelson

CTS 09-23

Technical Report Documentation Page

1. Report No. CTS 09-23	2.	3. Recipients Accession No.
4. Title and Subtitle Superbus Phase I: Accessory Loads Onboard a Parallel Hybrid-Electric City Bus		5. Report Date August 2009 6.
7. Author(s) Jeffrey Campbell, David Kittelson		8. Performing Organization Report No.
9. Performing Organization Name and Address Mechanical Engineering University of Minnesota 111 Church St. SE Minneapolis, MN 55455		10. Project/Task/Work Unit No. 11. Contract (C) or Grant (G) No. (C) (wo)
12. Sponsoring Organization Name and Address Center for Transportation Studies 200 Transportation & Safety Building 511 Washington Ave SE Minneapolis, MN 55455		13. Type of Report and Period Covered Final Report 01/08 - 06/09 14. Sponsoring Agency Code

15. Supplementary Notes
http://www.cts.umn.edu/Publications/ResearchReports/

16. Abstract (Limit: 250 words)

This paper describes the results from the first phase of the Superbus Project, which explores the input power trends and dependencies of the major accessories on a parallel hybrid urban transit bus. More specifically, this paper examines the elimination of both “accessory overdrive”, where more power is delivered to an accessory than is required by the function, and “parasitic loading”, where the accessory consumes power with no useful output. The bus was equipped with an array of sensors and a programmable data acquisition system (DAQ), and was driven on routes in Minneapolis during August and September, 2008. The accessories analyzed were the hydraulic pumps, the air compressor, the alternator, and the air conditioning system. Collection and processing methods are described, and the influence of accessory overdrive and parasitic loading are demonstrated.

The average input power to the accessories was 11.0 kW when the air conditioning was off and 19.3 kW when the air conditioning was on. By removing the effects of accessory overdrive and parasitic loading, it is estimated that replacing mechanically driven accessories with their electrically driven counterparts would reduce the accessory power demand by 34% (no air conditioning) and 31% (with air conditioning). Under the somewhat conservative assumption that with the air conditioning on, 50% of the bus’ fuel is consumed by its accessories, it is estimated that accessory electrification would result in a 13-15% improvement in overall fuel economy.

17. Document Analysis/Descriptors Vehicle components, hotel, loads, hybrid vehicles, public transit, buses, air conditioning systems, fuel conservation		18. Availability Statement No restrictions. Document available from: National Technical Information Services, Springfield, Virginia 22161	
19. Security Class (this report) Unclassified	20. Security Class (this page) Unclassified	21. No. of Pages 35	22. Price

Superbus Phase I: Accessory Loads Onboard a Parallel Hybrid-Electric City Bus

Final Report

Prepared by

Jeffrey S. Campbell
David B. Kittelson

Department of Mechanical Engineering
University of Minnesota

August 2009

Published by

Center for Transportation Studies
University of Minnesota
200 Transportation and Safety Building
511 Washington Avenue S.E.
Minneapolis, MN 55455-0375

Acknowledgements

The authors would also like to thank Metro Transit, the Initiative for Renewable Energy and Environment (IREE) and the Center for Transportation Studies (CTS) at the University of Minnesota for their financial support. In addition, the authors would like to thank Jan Homan, Chuck Wurzinger, and David Haas from Metro Transit, and Jake Swanson from the Center for Diesel Research for their extraordinary efforts in this project.

Table of Contents

List of Tables

List of Figures

Nomenclature

P_{in}	Input Power
ω	Rotational Speed
Vol	Displacement Volume
η	Efficiency
I	Current
V	Voltage
ECU	Engine Control Unit
APU	Auxiliary Power Unit

Executive Summary

In recent years, environmental concerns, fuel prices, and emissions regulations have pushed the public transit industry to invest in hybrid vehicles worth more than half a million dollars per unit. These state-of-the-industry hybrid buses have been designed to reduce fuel consumption by scavenging a portion of the energy spent on propulsion. As propulsion fuel consumption has decreased and demand for accessory loads such as air conditioning and electronic lighting/signs has increased, hybrid buses on urban routes in warm weather frequently spend more fuel on accessories than they do on locomotion. In other words, modern hybrid buses operated in warm weather have become more of a diesel-powered hotel on wheels than a vehicle with accessories. Despite their heavy "hotel" loads, the accessory powering scheme on today's parallel hybrid buses is primitive and poorly-controlled when compared to their hybridized drivetrains. The Superbus project takes a piecewise approach in the development of an advanced "big picture" strategy to improve the accessory powering scheme and reduce accessory fuel consumption on such parallel hybrid buses. This paper reports on the first phase of the project: an energy audit on the major accessories and an estimation of the effect of accessory electrification.

After conducting background research on accessory electrification, hybrid buses, and auxiliary power units, accessory performance data that allowed the calculation of accessory input torque values from other parameters (pressure, current, temperature, etc.) were collected from the manufacturers of the air compressor, the tandem hydraulic pump, the alternator, and the air conditioning system. The engine speed was also monitored and, through gear ratios to each accessory, was used to calculate the rotational speed of the accessories. With the ability to calculate instantaneous accessory input torque and RPM, input power for each accessory could be calculated.

A scheme was devised to collect the required parameters, then sensors and an on-board data acquisition system were purchased, programmed, and tested before being installed on the bus. Data was collected over a variety of routes, weather, traffic, and load conditions in August and September of 2008. Input power measurements and dependencies were analyzed for each accessory, and losses caused by the inability of the accessories to decouple their output from the engine's rotational speed were approximated. Such losses are divided into two groups:

I. <u>Accessory Overdrive:</u> where more power is delivered to an accessory than is required by the function, and

II. <u>Parasitic Loading:</u> where the accessory consumes power with no useful output.

Because electrical generators have the ability to decouple the engine speed from the generator output, these are problems that electrically driven accessories avoid all together.

It was calculated that when the air conditioning was off, the accessories on board the bus consumed a collective average of 11.0 kW and, when the air conditioning was on, the accessories consumed a collective average of 19.3 kW. By eliminating accessory overdrive and parasitic loading from the calculations (and therefore estimating the effect of accessory electrification), the average accessory power consumption was estimated to be reduced by 36% (with air conditioning) and 31% (without air conditioning). This result is slightly higher than BAE System's experimental results on a series hybrid bus, which estimated a 25% reduction in average accessory fuel consumption (with air conditioning) through accessory electrification on routes through New York City.

Under the somewhat conservative assumption that 50% of the engine's output is consumed by accessories when the air conditioning is on, accessory electrification is estimated to yield 13% (AC off) and 15% (AC on) improvement in overall fuel economy. This is consistent with the 5-10% improvement in fuel economy found by Page et al. when just the hydraulic engine cooling system was replaced with its electrically driven counterpart on a standard diesel bus.

1. Introduction

Three common paths to energy conservation in heavy duty vehicles are:

- Hybrid Drivetrains: Much of the heavy duty market for hybrid vehicles is in urban transit. In the 1980s, hydraulic hybrid buses showed a 66-86% improvement in fuel economy over diesel models of the same era [1, 2]. In the last half decade, bus manufacturers developed electric hybrid models that showed a 10% to 75% improvement in fuel economy over their modern diesel counterparts. [3-5].
- Optimization of Accessory Power Production: Depending on the duty cycle, it is not uncommon for accessory fuel consumption of heavy duty trucks and buses to exceed propulsion fuel consumption. In addition to added maintenance and engine wear, in recent years, semi truck fleet managers spent $1500 to $5000 per year per truck on fuel consumed at idle [6, 7]. Since then, the industry has begun to power accessories with small diesel engines called “auxiliary power units” (APUs) which, operated near peak efficiency, produce power more efficiently than the main engine at idle. Fuel cell APUs have also been experimentally demonstrated, but have made little impact in industry [8-12]. Simulation of a variety of APU technologies have shown a 3-15% overall fuel savings on semi trucks [13, 14]. Simulations done for fuel cell APUs on a medium duty Army tactical vehicle resulted in an 86% increase of idling fuel economy and a 20% increase in overall fuel economy [15, 16]. A fuel cell APU installed on a semi truck showed a 50% to 80% improvement in idling fuel economy compared to the main engine driven accessories [17]. In addition to the financial incentive to drive accessories more efficiently, environmental concerns have given rise to government restrictions. Local and statewide idling restrictions have been imposed in 23 states as of July 2008 [18].
- Optimization of Accessory Power Consumption: Electrification of heavy duty vehicle accessories has been shown to increase fuel economy by decoupling accessory output from engine speed, thereby improving accessory controls. In semi trucks, a large scale simulation of accessory electrification resulted in a 2.4-9.2% increase in fuel economy [19]. Replacing a mechanically driven engine cooling system with its electrically driven counterpart showed overall fuel savings of 5-20% for an Army tactical vehicle and 5-10% on an urban transit bus [20, 21].

The Superbus Project aims to combine the above fuel-saving strategies for a parallel hybrid urban transit bus. The three phases of the project are:

1. Analysis of accessory performance, accessory overdrive, and parasitic loading
2. Selective replacement of mechanically driven accessories with electrically driven counterparts
3. Implementation of a fuel cell APU to drive electric accessories.

This paper reports on Phase 1, the testing portion of which was performed in August and September of 2008.

Apparatus and Methods

2.1. General

The bus used for this project is a parallel electric hybrid transit bus purchased by Metro Transit of Minneapolis/St. Paul in March, 2008. Table 1 shows basic bus specifications.

Figure 1: The Bus

Table 1: Bus Specifications

Curb Weight:	29,550 lbs (13,400 kg)
Length	41.5 ft (12.6 m)
Width	8.3 ft (2.5 m)
Height/Height with Battery	9.0 ft/10.5 ft (2.7 m/3.0 m)
Wheelbase	23.3 ft (7.1 m)
Engine Type	2007 Cummins ISB
Rated Torque	620 lbf-ft (841 Nm) @ 1600 RPM
Rated Power	260 HP (194 kW)
Hybrid Drive System	Allison EP40
Passenger Capacity	38 seated, 28 standing

Because accessory input power measurements were difficult to perform while the bus was in service, performance data provided by the accessory manufacturers was used to estimate input power using other parameters. These parameters were collected and stored using an array of sensors and a Compact Field Point (cFP) data acquisition system. The cFP was installed on the curb side of the AC system compartment and is shown in Figure 2.

Figure 2: Compact FieldPoint Data Acquisition System

The accessories analyzed in this project are listed below and shown schematically in Figure 3:

- A tandem hydraulic pump (power steering, engine fan)
- Air compressor
- Air conditioning (AC) compressor
- Alternator

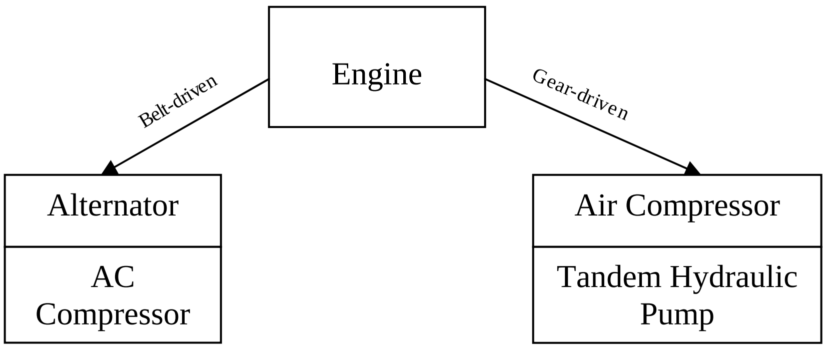

Figure 3: Accessory Schematic

The cFP and sensors were powered by the bus's 12V line. A LabVIEW™ Real-Time program was developed for the cFP to poll and store coordinated readings from each of the sensors at a rate of 1 Hz, and data files were stored on a USB mass storage device. A GPS unit was installed on the roof of the bus to monitor latitude, longitude, and velocity of the bus.

The following sections provide engine and accessory descriptions, sensor information, and methods for calculating accessory input power using manufacturer performance data.

2.2. Engine

Engine bay geometry made it difficult to directly measure the rotational speed of the engine's crankshaft, so an optical sensor measured the rotational speed of an idler belted to the crankshaft, as shown in Figure 4. The idler speed was converted to crankshaft speed using a gear ratio. The gear ratio between the crankshaft and each accessory was known, so this idler RPM measurement was also used to calculate the rotational speed of each accessory. It was assumed that there was no belt slip. A Controller Area Network (CAN) reader was used to log engine torque and RPM from the engine control unit (ECU).

Figure 4: Idler and Optical Sensor

2.3. Hydraulic Pumps: Engine Fan and Power Steering

The hydraulic system consists of two circuits. The displacements of the gear-type pumps and motors are listed in Table 2.

Table 2: Displacement Volume of Hydraulic Pumps and Motors

Circuit	Pump Displacement (cc)	Motor Displacement (cc)
Engine Fan	41	44
Power Steering	19	Unknown

The power steering circuit is a closed loop between the pump and motor with a bypass valve across the motor. The engine fan circuit consists of the same loop, but includes a hydraulic cooler and a more complex motor bypass control scheme. Neither the cooler nor the control scheme is an obstacle to analysis, as only the input power to the pumps is under consideration. Both circuits are shown in Figure 5.

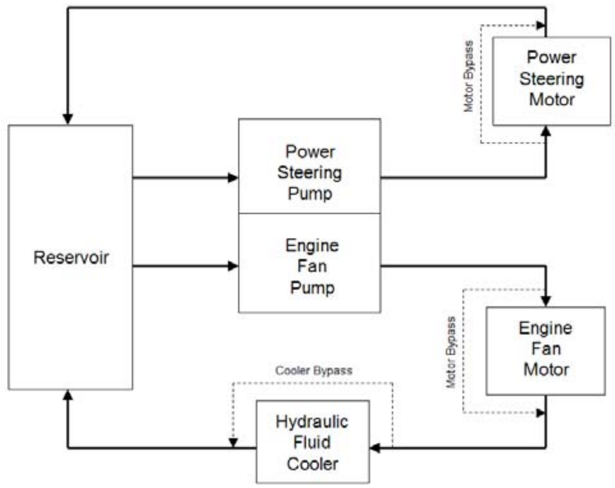

Figure 5: Hydraulic System Diagram

The suction sides of these pumps draw fluid from a vented reservoir, assumed to be at atmospheric pressure. Transducers measured pressure on the high pressure side of the pumps. For each pump, the manufacturer provided an estimate of mechanical efficiency given the rotational speed and pressure differential. Together with the displacement volume (Table 3), these parameters were used to calculate the instantaneous power input of each hydraulic pump using Equation 1.

$$P_{in} = \frac{\omega * Vol * \Delta P}{\eta_{mechanical}} \qquad (1)$$

2.4. AC Compressor

The air conditioning system on board the bus has a rated capacity of 32 kW (110,000 BTU/hr). The AC compressor is a screw-type system equipped with two loading valves which reduce the displacement volume by approximately 1/3 and 2/3 when engaged. Electrical signals controlling the clutch and loading valves were logged by the cFP. Thermocouples were placed in the AC condenser inlet (ambient air above the bus), the AC evaporator inlet (passenger cabin), and the AC evaporator outlet (cooled air input to the passenger cabin). Readings from these thermocouples were used to estimate input power from manufacturer performance data and to ensure that the air conditioning system was working properly.

The AC compressor manufacturer provided a single graph which, with the RPM and condenser inlet temperature known, estimated the input power to the AC compressor at full volume. To estimate the 1/3 and 2/3 volume conditions, the full volume input power was multiplied by 1/3 and 2/3, respectively. While this does not account for the fairly constant friction losses in the lower load levels, the manufacturer recommended it as a first-pass estimation for the infrequently used 1/3 and 2/3 load states.

2.5. Air Compressor

The intake air pressure of the piston-type air compressor was measured with a pressure transducer. A second transducer was placed in the air compressor's governor line. The pressure in the governor line signaled whether the air compressor was "loaded" or "unloaded". The manufacturer provided graphs of input power vs. RPM over a wide array of inlet air pressures in both the "loaded" and "unloaded" states.

2.6. Alternator and Electric AC Fans

To power AC fans and other electronics, the bus utilized a brushless 280A @ 24V (nominal) alternator. Although no on-the-road voltage measurements were performed, the alternator output and the AC fan input were measured to be 27.3V at both slow idle and fast idle. Loading valve controls on the AC compressor also read 27.3V. These measurements were all assumed to be constant. The instantaneous current output of the alternator was measured using a current sensor clamp, shown applied to the alternator output wire in Figure 6.

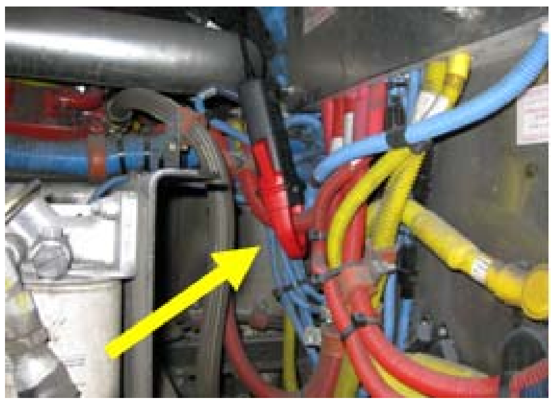

Figure 6: Alternator Current Sensor

The alternator manufacturer supplied a map of efficiency versus alternator RPM at peak load. As a means to estimate efficiency at non-peak load, the manufacturer included a zero-current to full-current efficiency profile at a single intermediate RPM value. This curve, shown in Figure 7, was normalized and applied to all RPM values.

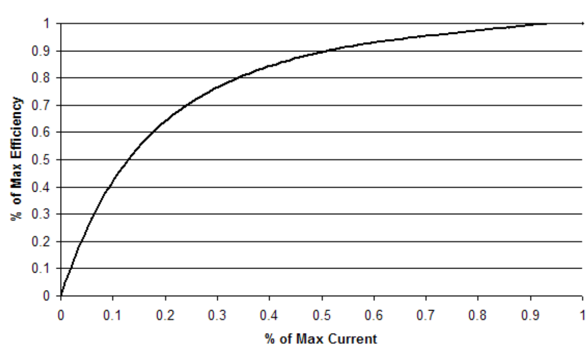

Figure 7: Alternator Efficiency Normalization

Using full load data together with Figure 7, an estimation of alternator input power can be made using Equation 2.

$$P_{in} = \frac{V * I}{\eta_{alternator}} \qquad (2)$$

A second current sensor was clamped onto the electrical input to the air conditioning fans to monitor their current draw. While the AC fans are powered by the alternator, and therefore provide no unique load on the engine, they do have a substantial influence on the alternator’s output and efficiency. This will be further examined in Section 3.7.

3. Results

3.1. General

Table 3 shows data collection dates, time, and duration. Collection duration is shorter than the difference between the start and stop times, as breaks occurred for driver changes, schedule corrections, refueling, and layovers.

Table 3: Operation Details

Date	Start , Stop Times	Collection Duration (hours)
Aug 27th	04:32 - 24:08	16.5
Aug 28th	05:50 - 25:55	18.2
Aug 29th	12:25 - 23:11	9.9
Aug 30th	17:24 - 26:15	7.0
Aug 31st	07:27 - 23:17	15.5
Sept 1st	05:40 - 25:12	18.2
Sept 2nd	07:30 - 19:19	6.2
Sept 3rd	05:50 - 19:19	12.6
Sept 4th	05:31 - 25:29	17.9
Sept 5th	14:13 - 19:26	13.3
Sept 8th	06:23 - 19:22	10.3
Total	x	145.6

The duty cycle for an urban bus varies widely depending on the location, routes, and time of day. A common metric of comparison is the velocity profile. Figure 8 and Figure 9 show the histogram and cumulative histogram of bus velocity for all eleven days of collection.

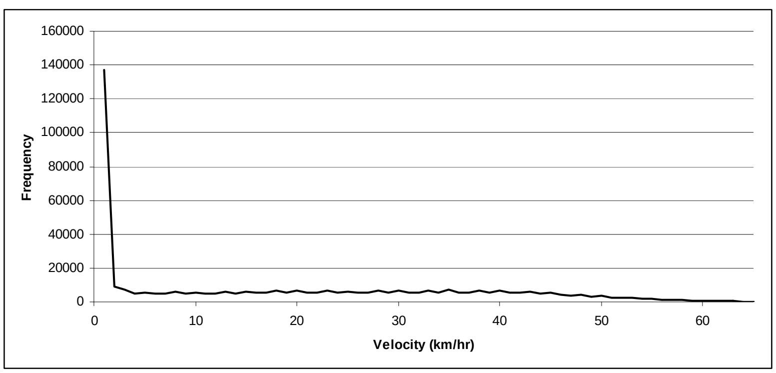

Figure 8: Bus Velocity Histogram

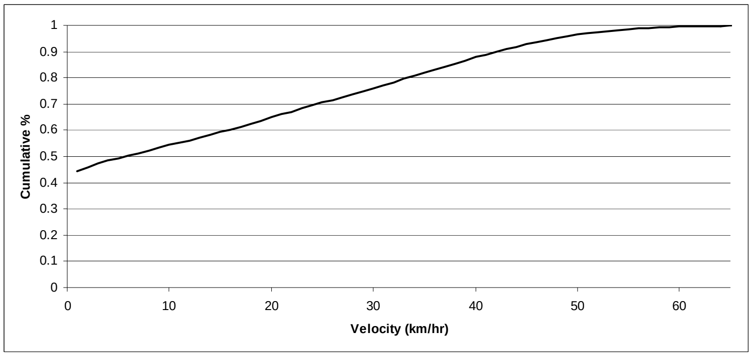

Figure 9: Cumulative Bus Velocity Histogram

The GPS falsely reported many zero values to be slightly larger than zero. Under the assumption that readings under 1 km/hr were 0 km/hr, 44% of the engine's run time was spent driving accessories at rest. The mean velocity of the bus was 16.1 km/hr, and the median velocity was 7.8 km/hr.

3.2. Engine

A Controller Area Network (CAN) reader was used to log engine torque and RPM from the engine control unit (ECU). At slow idle with the AC system off, the CAN reported an engine output power of 6.5 kW; within 8% of the total accessory input power estimations (7.0 kW). The total accessory load increased by 5.8 kW to 12.8 kW when the AC system was turned on. The engine output power, however, increased by only 0.3 kW to 6.8 kW. Now, the discrepancy between engine output (6.8 kW) and accessory input (12.8 kW) was 88%. The engine RPM readings from the ECU were confirmed by the optical sensor on the engine idler. Furthermore, it was known that the idling 32 kW AC system at full volume consumed far more than the 0.3 kW registered by the ECU. It was therefore determined that the engine torque readings were inaccurate, so they are not included in this study.

While the bus velocity informs the duty cycle of the bus, the data in this report shows that the strongest dependency of mechanically driven accessories is often the engine speed.

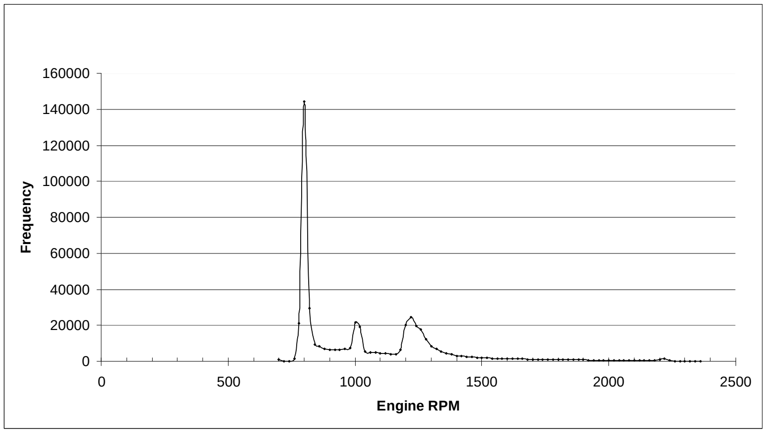

Figure 10: Engine RPM Histogram

Figure 10 shows three steady state RPM regimes. The spikes near 775 RPM and 1000 RPM represent "slow idle" and "fast idle", respectively. The spike near 1250 RPM is the region where the hybrid controls hold the engine during acceleration. The presence of this triple spike in the accessory input power histograms that follow show qualitatively that the accessory's performance is strongly dependant on engine speed.

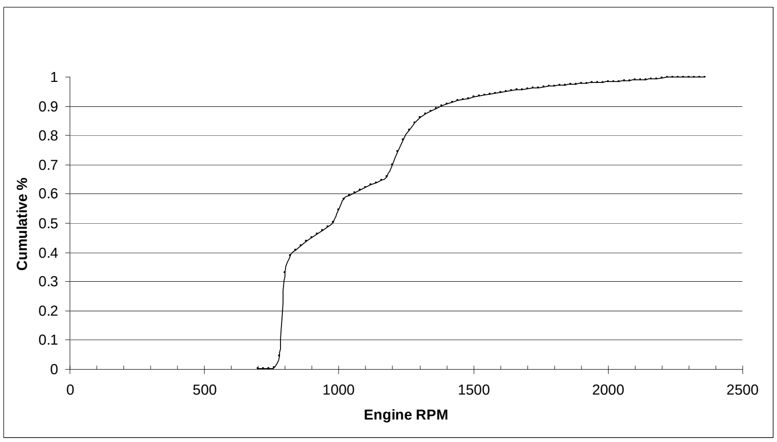

Figure 11: Cumulative Engine RPM Histogram

Slow idle is the speed most commonly experienced by the accessories. Figure 11 shows that the engine is running at slow idle (< 820 RPM) for 39% of the engine's run time.

3.3. Engine Fan Pump

Figure 12 shows the time series of the power consumption of the engine fan pump during one day of service.

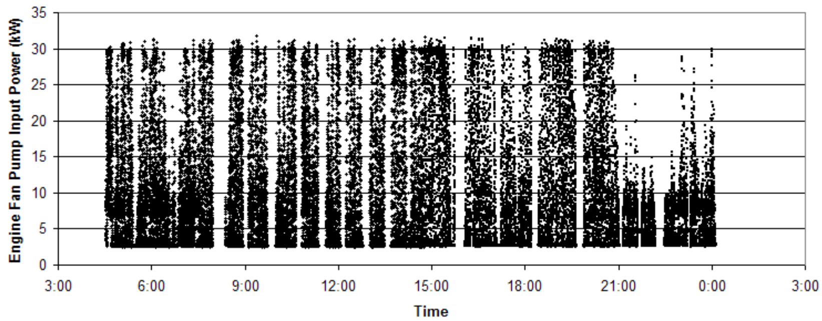

Figure 12: Engine Fan Input Power Time Series

While a time series shows minima, maxima, and operation times, a more informative representation of the power consumption dependencies is the shown in Figure 13.

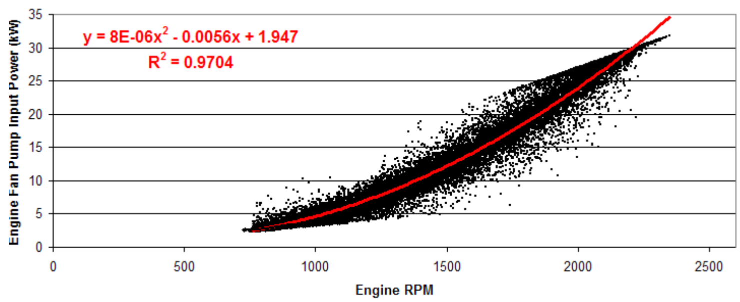

Figure 13: Engine Fan Pump Input Power vs. Engine RPM

While the need for heat rejection does increase with engine speed, cooling power demand is typically linearly related to engine speed. Figure 13 shows that, as the rotational speed triples from idle to maximum speed, the input power to the engine fan pump increases nearly ten-fold in a polynomial fashion. It is therefore strongly suspected that, at high engine speed, more power is being delivered to the pump than is needed. This excessive delivery of power to an accessory is referred to as “accessory overdrive”.

The final unique feature of Figure 13 is the linearly increasing cap of input power readings imposed at engine speeds above 1700 RPM. This cap is a product of the engine fan circuit’s controls, which releases system pressure in excess of 16.5 MPa. With the pressure held constant, engine speed is the only parameter allowed to influence input power, resulting in a linear input power cap as engine speed increases. Figure 14 shows how pressure differential varies with engine speed.

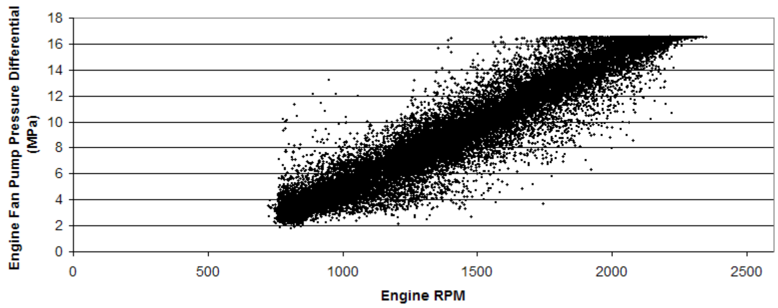

Figure 14: Engine Fan Pump Pressure Differential vs. Engine RPM

The characteristic "triple spike" in Figure 14 once again illustrates the engine fan pump's strong dependence on engine speed. The mean input power to the hydraulic fan pump is 6.4 kW, and the median input power is 4.4 kW.

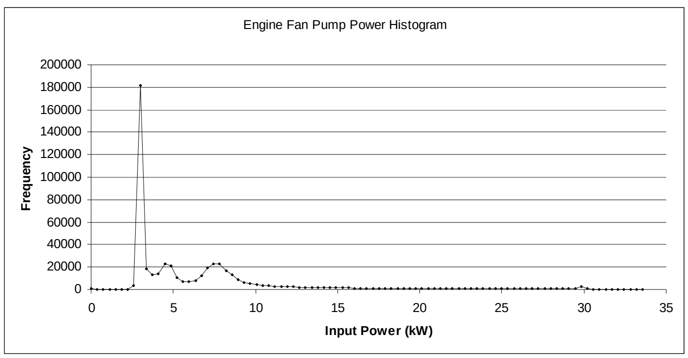

Figure 15: Engine Fan Input Power Histogram

3.4. Power Steering Pump

Similar to the engine fan circuit, the power input to the hydraulic pump on the power steering circuit has a strong dependence on engine speed. However, more influential than the engine speed are the rapid increases in pressure differential across the pump as the steering wheel is turned. Generally speaking, the driver turns the bus more frequently when the bus is traveling slowly. Moreover, when then bus is moving slowly, the engine tends to also run at low and intermediate speeds. As a consequence, these sharp pressure spikes occur most frequently at low and intermediate engine speeds. Figure 16 shows the how pump pressure differential and engine speed influence the input power to the power steering pump.

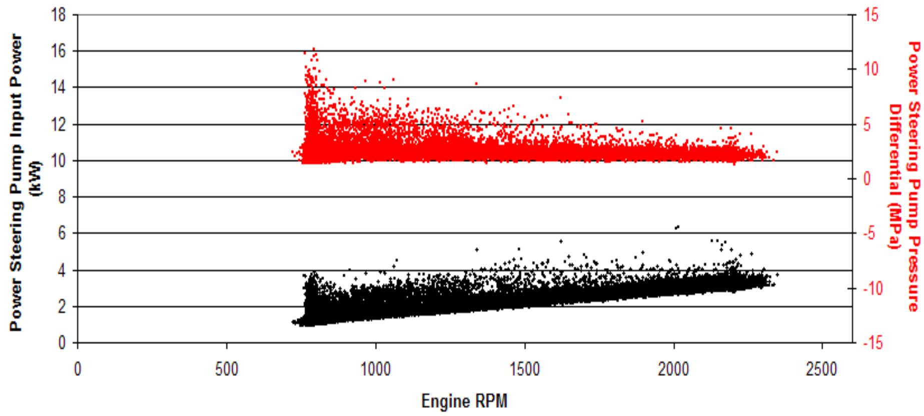

Figure 16: Power Steering Input Power, Pressure Differential vs. Engine RPM

All flow in excess of 15 liters per minute through the power steering circuit is sent through a motor bypass. With a pump displacement of 19cc, this flow rate is reached at approximately 800 RPM, or "slow idle". Therefore, whenever the engine operates at rotational speeds greater than 800 RPM, there is accessory overdrive. Although it was not quantified in this study, there is also "parasitic loading", where the pump is doing work when there is no need for the function. Though it is neither parasitic loading nor accessory overdrive, an additional source of energetic waste is inefficient pressure and RPM range in which the power steering pump is operated; with an average efficiency of 45%, the power steering pump operates well short of its peak efficiency of 81%.

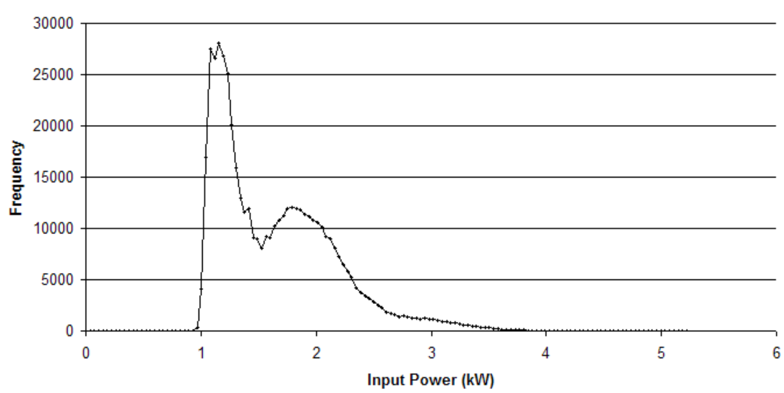

Figure 17: Power Steering Pump Input Power Histogram

Figure 17 is the histogram of input power to the hydraulic pump on the power steering circuit. The characteristic triple spike found in the engine fan's hydraulic pump is reduced to only two peaks in the power steering circuit for two reasons.

1. Pressure spikes at low and intermediate engine speeds cause sharp increases in input power, diluting the correlation between engine RPM and input power.
2. The difference in input power between the 1000 RPM and 1250 RPM regimes is small (see Figure 16).

Thus, the wide spike found between 1.5 and 2.5 kW consists pressure spikes at low engine speeds together with the base 1000 RPM and 1250 RPM idle conditions. The mean input power to the power steering pump is 1.6 kW, and the median input power is 1.5 kW.

3.5. AC Compressor

The top cluster of long lines in Figure 18 shows the fully-loaded condition, with the different bands representing different ambient temperatures. The small, lower clusters represent the less common 1/3 and 2/3 displacement volume conditions. Because the AC compressor data were processed without temperature interpolations, the input power calculations in Figure 18 are shown in discrete lines. The error introduced by this lack of temperature interpolations for the full load condition was calculated as half of the difference between adjacent lines at a given engine speed, and is tabulated at different engine speeds in Table 4.

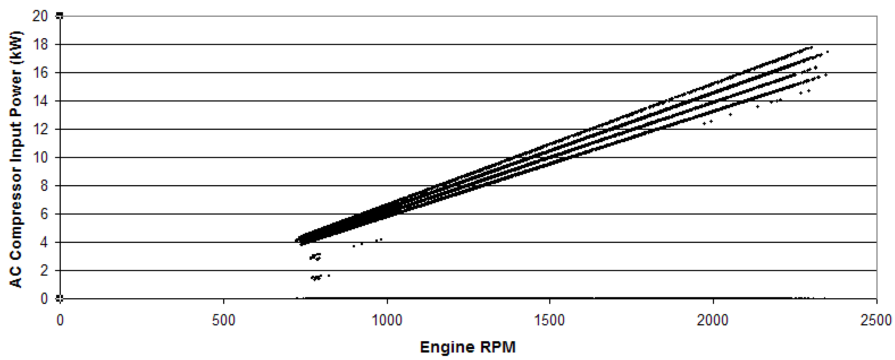

Figure 18: AC Compressor Input Power vs. Engine RPM

Table 4: Full-load Error in AC Compressor Input Power

RPM	Error
775 RPM (slow idle)	<0.1 kW
1600 RPM	0.2 kW
2300 RPM (max RPM)	0.4 kW

Because the demand for AC cooling is largely independent of engine speed, the tripling of input power from low idle to maximum engine speed is strong indicator of accessory overdrive. Table 5 details the relative frequency of the different volume- and therefore load-conditions.

Table 5: Daily Air Conditioning Performance

Date	Hours of Data Collection	Time at No Load	Time at 1/3 Load	Time at 2/3 Load	Time at Full Load	Peak Temp (ºC)	Average Temp (ºC)
Aug 27th	16.5	100%	0%	0%	0%	29	22
Aug 28th	18.2	57%	<1%	5%	38%	32	22
Aug 29th	9.9	20%	<1%	2%	78%	36	28
Aug 30th	7.0	52%	<1%	<1%	48%	38	26
Aug 31st	15.5	25%	<1%	<1%	75%	37	28
Sept 1st	18.2	23%	<1%	3%	74%	39	29
Sept 2nd	6.2	95%	<1%	<1%	5%	29	21
Sept 3rd	12.6	50%	<1%	49%	1%	29	27
Sept 4th	17.9	91%	<1%	6%	2%	23	17
Sept 5th	13.3	76%	<1%	2%	22%	29	19
Sept 8th	10.3	100%	0%	0%	0%	28	18
Total	**145.6**	**61%**	**<1%**	**6%**	**32%**	**39**	**23**

The 1/3 load condition is primarily used as a transition from a zero load to a higher load. The 2/3 load condition behaves as a transitional point as well, but it is also occasionally used in steady state operation. On September 3rd, for example, the 2/3 load condition was used for 49% of the day's collection time. This long-term application is likely due to the day's moderate and steady temperature (27ºC average, 29ºC max) where a constant, small cooling load was needed to bring the cabin to a comfortable temperature.

Figure 19 is a histogram of the input power to the AC compressor. The 1/3 and 2/3 load conditions are combined in red, and the full load condition is shown in black.

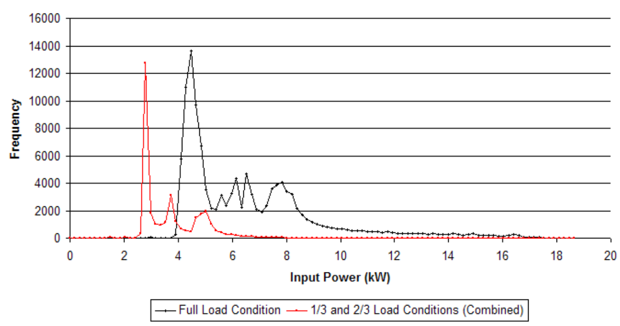

Figure 19: AC Compressor Input Power Histogram

The characteristic "triple spike" in Figure 19 illustrates the AC compressor's dependence on the engine's rotational speed. The compressor has no means to completely decouple its output from the engine's rotational speed to eliminate accessory overdrive. However, by reducing the pump's displacement volume by a factor of 1/3 or 2/3 when full load is not needed, the AC compressor controls are effective in reducing the impact of accessory overdrive. The mean input power to the AC compressor is 6.1 kW and the median is 5.2 kW.

3.6. Air Compressor

Figure 20 shows a plot of input power vs. engine RPM for the air compressor.

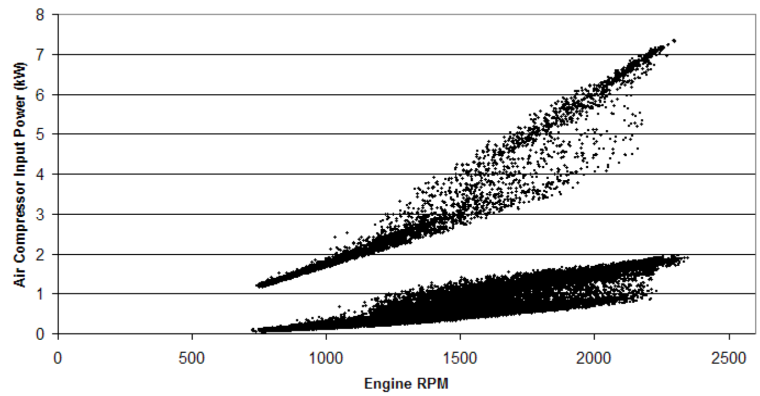

Figure 20: Air Compressor Input Power vs. Engine RPM

The top cluster of data points represents the "loaded" state, where the compressor is working to add air to the tanks. The bottom cluster is the "unloaded" state, where the air compressor spins with the inlet valve left open. With 84% of the engine's run time spent in this unloaded state, the air compressor experiences substantial parasitic loading. During the course of this audit, for every 1 kW spent pumping air into the tanks, 1.03 kW was spent in parasitic loading.

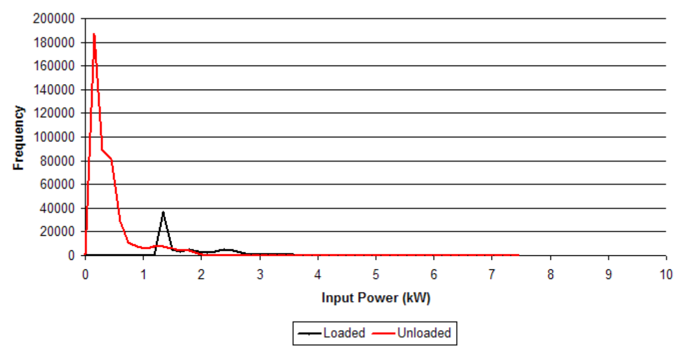

Figure 21: Air Compressor Input Power Histogram

Figure 21 is the histogram of the air compressor's two states. In the loaded state, the mean input power is 1.9 kW and the median is 1.5 kW. In the unloaded state, the mean input power is 0.33 kW and the median is 0.19 kW. The overall mean input power is 0.58 kW and the median is 0.27 kW.

3.7. Alternator and Electric AC Fans

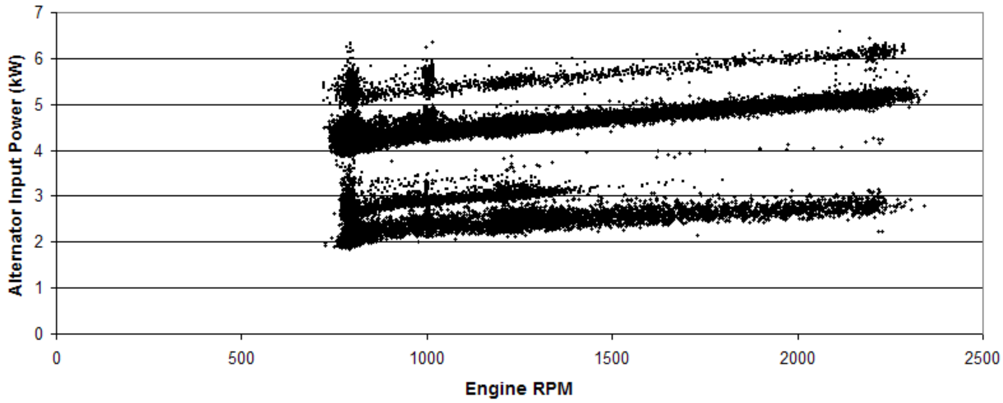

Figure 22: Alternator Input Power vs. Engine RPM

Figure 22 shows a plot of alternator input power vs. engine RPM in several bands, each showing an increase in input power as engine RPM increases. However, unlike the results found in the hydraulic systems and the AC compressor, this increase in input power is not a sign of accessory overdrive. Among the accessories analyzed in this study, the alternator is unique in its ability to maintain a constant output power for a given load level, regardless of engine speed. The independence of output power from engine speed is demonstrated in Figure 23.

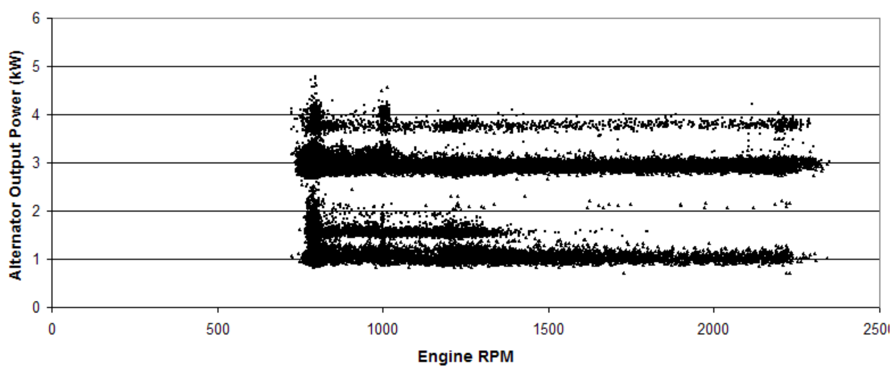

Figure 23: Alternator Output Power vs. Engine RPM

Figure 24 shows the reason for an increase in alternator input power while the alternator's output power remains constant. As engine speed increases, the alternator efficiency decreases appreciably in each band. It is important to note that this change in efficiency does not represent accessory overdrive, as the output of the alternator remains constant in each load level.

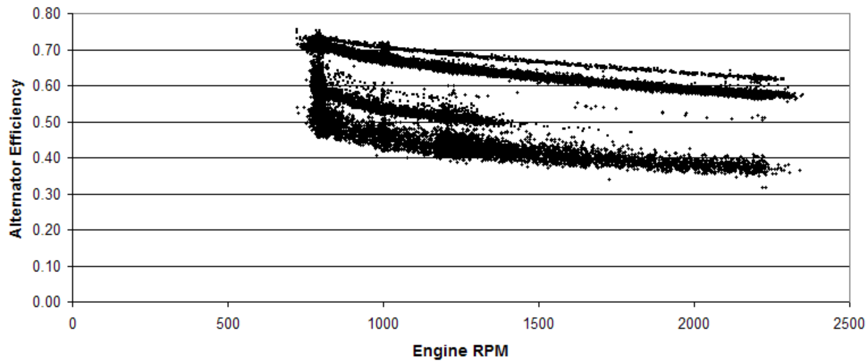

Figure 24: Alternator Efficiency vs. Engine RPM

The AC fans have considerable influence on alternator performance and efficiency because they are the largest electrical load. Figure 25 quantifies the five discrete AC fan loads (including "off"), which are responsible for the banding phenomenon present in Figures 22-24. The relative frequency of these settings is shown in Figure 26.

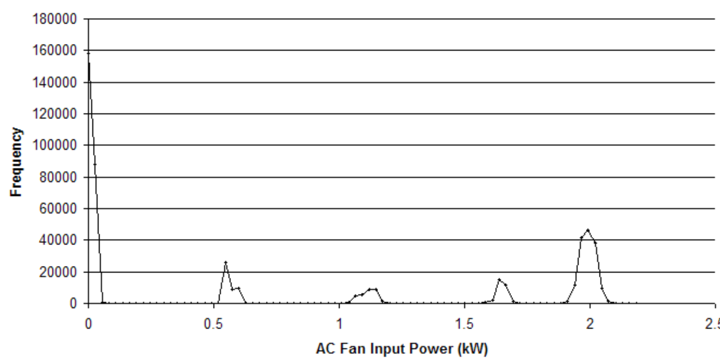

Figure 25: AC Fan Input Power Histogram

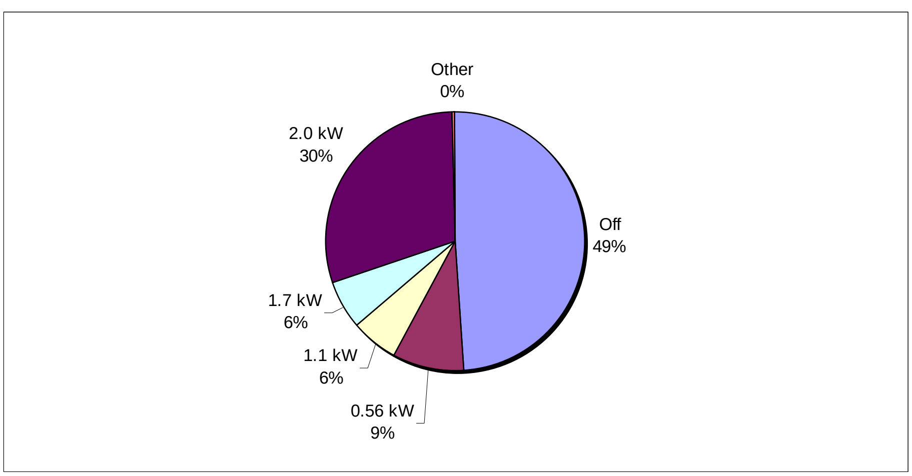

Figure 26: Relative Frequency of AC Fan Power Settings

Figure 27 shows distinct peaks in the alternator input power histogram. In contrast to the other accessories, these spikes are not due to a strong dependence on engine speed. Rather, the spikes near 2.5 kW and 4.5 kW represent the two most frequent AC fan operating conditions (AC fans off and AC fans at full power). When the AC fans are off, the average input power to the alternator is 2.3 kW. When the fans are on, the weighted average of input power is 4.5 kW. More information on alternator loading can be found in Table 6.

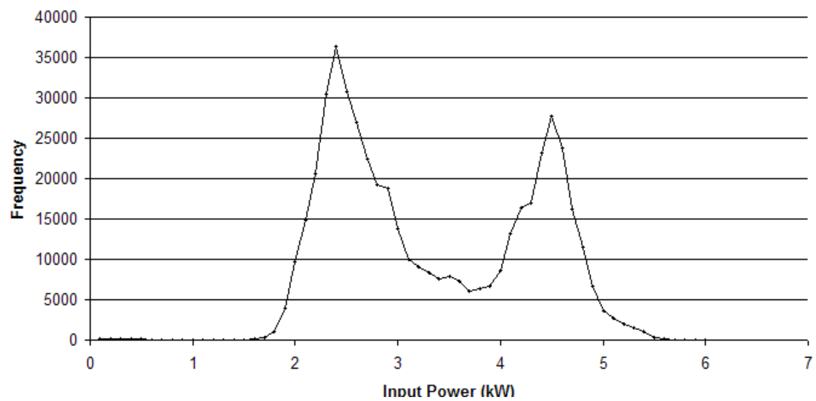

Figure 27: Alternator Input Power Histogram

Table 6: Effect of AC Fans on Alternator Output and Performance

	Alternator Efficiency @ idle	**Average Non-AC Fan Input Power (kW)**	**Average AC Fan Input Power (kW)**	**Average Total Alternator Input Power (kW)**
AC off	45% - 55%	2.3	0	2.3
AC on	55% - 75%	1.6	2.9	4.5

3.8. Overall

Figure 28 and Figure 29 show the relative magnitudes of average accessory loads. When the AC is off, the engine fan pump is responsible for 57% of the total accessory load. When the AC is on, the engine fan pump is 33% of the accessory load while the AC system (AC compressor and AC fans) account for 47%. Overall, the AC system and the engine fan pump dominate the accessory loading on the engine. Combined with their susceptibility to accessory overdrive, the large power demands of the AC compressor and engine fan pump make them especially strong candidates for replacement by electrically driven counterparts. This is explained further in the discussion of Table 7.

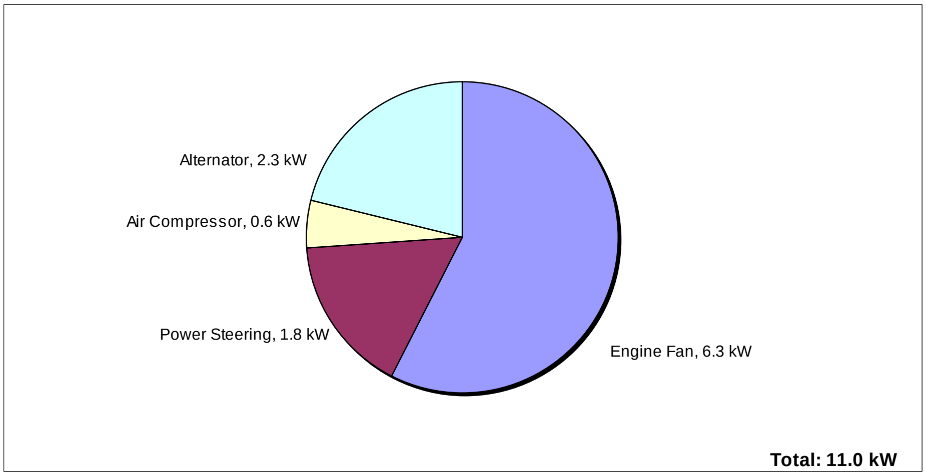

Figure 28: Average Accessory Input Power (kW): Air Conditioning Off

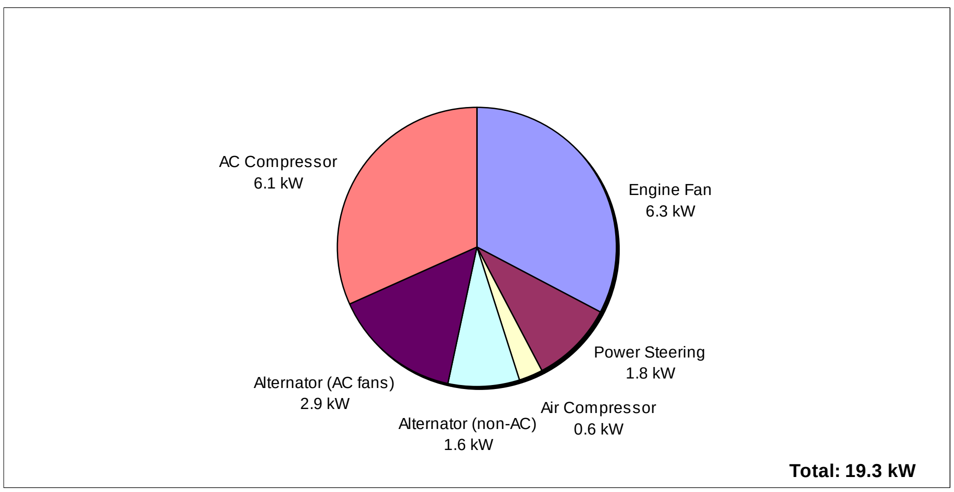

Figure 29: Average Accessory Input Power (kW): Air Conditioning On

As a first step toward predicting fuel savings in electrification of all analyzed accessories, the following assumptions are considered:

1. All electrically driven accessories operate only at the “idle” power input of their mechanically driven counterparts.
2. This idle condition provides enough power to perform the accessory’s function at all times, and
3. Each accessory is given a means to decouple itself from the engine’s rotational speed when its function is not needed

Under these assumptions, accessory loading is well quantified, and both accessory overdrive and parasitic loading are eliminated. The average input power for each accessory from Figure 28 and Figure 29 is repeated in Table 7 along with a “theoretical” average input power if the above assumptions are considered.

Table 7: Primary Effects of Eliminating Accessory Overdrive and Parasitic Loading

	Original Average Input Power (kW)	**Theoretical Average Input Power (kW)**	**Average Load Reduction (kW)**	**Average Load Reduction (%)**
Engine Fan Pump	6.3	3.2	3.1	49%
Power Steering Pump	1.8	1.2	0.6	34%
AC Compressor	0 / 6.1	0 / 4.1	0 / 2.0	33%
Air Compressor	0.58	0.29	0.29	50%
Alternator	2.3 / 4.5	2.3 / 4.5	0	0%
Total	**11.0 / 19.3**	**7.0 / 13.3**	**4.0 / 6.3**	**36% / 31%**

Note: The pairs of values in the "AC Compressor", "Alternator" and "Total" rows represent values for when the AC system is off and when it is on.

The theoretical average input power for the power steering pump is assumed to be the average of values when the engine speed is below 800 RPM, and does not consider a reduction of parasitic loading. Also, the value for the AC compressor input power is taken as the weighted average of the fully loaded, 2/3, and 1/3 loaded states. Accounting for other factors that positively and negatively influence the theoretical average input power in Table 7 are beyond the scope of this paper. For example, the engine fan would likely need more power than is provided at idle to cool a heavily-loaded engine. On the other hand, high capacity generator/electric motor systems typically operate at higher efficiencies than mechanically driven accessories at idle. The signage, lighting, and other basic electrical loads now handled by the 280A alternator, for example, would almost certainly provide for more efficiently with a large generator. The same could be said for an electric power steering motor operating more efficiently than the current hydraulic system.

As seen in the *Average Load Reduction (kW)* column of Table 7, when the AC is off, the engine fan accounts for 78% of the *Total Average Load Reduction*. When the AC is on, the engine fan (49%) and the AC compressor (32%) account for 81% of the *Total Average Load Reduction*. From these numbers, it is clear that the bulk of the load reduction found in the elimination of parasitic loading and accessory overload (78% AC off, 81% AC on) is attributed to the engine fan system and the AC compressor.

The *Total Average Load Reduction (%)* values of 36% (AC off) and 31% (AC on) are comparable to the 25% (AC on) reported by BAE Systems in their analysis of a recent model series hybrid bus on routes in Bronx, New York [22]. This same study showed that the accessories accounted for 60% of the bus's fuel consumption (with the AC on). As discussed in Section 3.2, engine torque data in this study was determined to be inaccurate, so it is not known what percent of the parallel hybrid's fuel was consumed by accessories. Overall fuel savings are calculated in Table 8, assuming accessories are responsible for 50%, 60%, and 70% of the bus's fuel consumption.

Table 8: Overall Effects of Eliminating Accessory Overdrive and Parasitic Loading

AC System	Average Accessory Input Power (kW)	% of fuel consumed by accessories (with AC on)	Average Propulsion Input Power (kW)	% Reduction in Accessory Fuel Consumption	Reduced Accessory Input Power (kW)	% Reduction in Overall Fuel Consumption
Off	11.0	50%	19.3	36%	7.0	13%
On	19.3			31%	13.3	15%
Off	11.0	60%	12.9	36%	7.0	17%
On	19.3			31%	13.3	19%
Off	11.0	70%	8.3	36%	7.0	21%
On	19.3			31%	13.3	22%

Using the somewhat conservative estimate of 50% accessory fuel consumption, the overall expected fuel savings of 13% (AC off) and 15% (AC on).These results are consistent with the 5-10% improvement found by Page et al. when just the engine cooling system was replaced with its electrically driven counterpart on a standard diesel bus [21].

4. Conclusion

During 11 days of testing, 145.6 hours of data was collected as a parallel electric hybrid bus conducted routes through Minneapolis during the late summer of 2008. Average input power values to the following accessories were calculated:

- Tandem hydraulic pump (power steering, engine fan)
- Air compressor
- Air conditioning (AC) compressor and AC fans
- Alternator

When the air conditioning was off, the accessories consumed a collective average of 11.0 kW and, when the air conditioning was on, the accessories consumed a collective average of 19.3 kW. Electrification of these accessories would eliminate both accessory overdrive and parasitic loading. By approximating the impact of eliminating accessory overdrive and parasitic loading, the average accessory power consumption was estimated to be reduced by 36% (with air conditioning) and 31% (without air conditioning). This result is slightly higher than BAE System's experimental results on a series hybrid bus, which estimated a 25% reduction in average accessory fuel consumption (with air conditioning) through accessory electrification on routes through New York City.

Under the somewhat conservative assumption that 50% of the engine's output is consumed by accessories when the air conditioning is on, electrification of accessories would result in a 13% (AC off) / 15% (AC on) improvement in overall fuel economy. This is comparable to a 5-10% improvement in fuel economy found by Page et al. when just the hydraulic engine cooling system was replaced with its electrically driven counterpart on a standard diesel bus [21]. If complete accessory electrification is not feasible, it is estimated that most of the fuel savings (78% AC off, 81% AC on) can be achieved by electrification of just the engine fan and AC compressor.

5. Future Work

The next phase of the Superbus Project replaces some or all of the mechanically driven accessories with electrically driven counterparts, estimates fuel savings, and compares them to the estimated savings in this report. The final phase of the project examines how to best generate the electrical energy needed to power the electrically driven accessories. One possibility is a properly sized fuel cell APU installed on the bus.

References

1. Slutsky, S. "Regenerative Braking in Diesel-Powered Urban Buses." *SAE Paper 841690* (1984).

2. Hagin, F. “Regenerative Braking for City Buses.” Proceedings of the Intersociety Energy Conservation Engineering Conference (Miami Beach, FL, 1985): p. 491-496.

3. Chiang, P.K., “Two-Mode Urban Transit Hybrid Bus In-Use Fuel Economy Results from 20 Million Fleet Miles.” *SAE Paper 2007-01-0272* (2007).

4. Hayes, R.R., Williams, A., Ireland, J., Walkowicz, K., Black, S., “King County Metro – Allison Hybrid Electric Transit Bus Testing.” *SAE Paper 2006-01-3570* (2007).

5. Barnitt, R.A., “In-Use Performance Comparison of Hybrid Electric, CNG, and Diesel Buses at New York City Transit.” *SAE Paper 2008-01-1556* (2008).

6. Stodolsky, F., Gaines, L., and Vyas, A., “Analysis of Technology Options to Reduce the Fuel Consumption of Idling Trucks.” *Argonne National Laboratory, Argonne, IL, ANL/ESD-43* (2000).

7. Grupp, D., Forrest, M., Mader, P., Brodrick, C.J., Miller, M., Dwyer, H., “Development of a Retrofit Fuel Cell Auxiliary Power Unit for Truck Idle Reduction.” *SAE Paper 2004-01-2629* (2004).

8. Zizelman, J., Shaffer, S., Mukerjee, S., “Solid Oxide Fuel Cell Zuxiliary Power Unit- A Development Update.” *SAE Paper 2002-01-0411* (2002).

9. Broderick, C.J., Farshchi, M., Dwyer, H.A., “Demonstration of a Proton Exchange Membrane Fuel Cell as an Auxiliary Power Source for Heavy Trucks.” *SAE Paper 2000-01-3488* (2000).

10. Grupp, D., Forrest, M., Mader, P., Broderick, C.J., Miller, M., Dwyer, H., “Development of a Retrofit Fuel Cell Auxiliary Power Unit for Truck Idle Reduction.” *SAE Paper 2004-01-2629* (2004).

11. Surampudi, B., Redfield, J., Ray, G., Montemayor, A., Walls, M., “Electrification and Integration of Accessories on a Class-8 Tractor.” *SAE Paper 2005-01-0016* (2005).

12. Redfield, J., Surampudi, B., Ray, G., Montemayor, A., “Accessory Electrification in Class 8 Tractors.” *SAE Paper 2006-01-0215* (2006).

13. Hendricks, T., O’Keefe, M., “Heavy Vehicle Auxiliary Load Electrification for the Essential Power System Program: Benefits, Tradeoffs, and Remaining Challenges.” *SAE Paper 2002-01-3135* (2002).

14. Lutsley, N., Wallace, J., Broderick, C.J., Dywer, H. A., Sperling, D., “Modeling of Stationary Power for Heavy-Duty Trucks: Engine Idling vs. Fuel Cell APUs.” *SAE Paper 2004-01-1479* (2004).

15. Conover, J., Husted, H., MacBain, J., “Logistics and Capability Implications of a Bradley Fighting Vehicle with a Fuel Cell Auxiliary Power Unit.” *SAE Paper 2004-01-1586* (2004).

16. Filipi, Z., Louca, L., Stefanopoulou, A., Pukrushpan, J., Kittirungsi, B., Peng, H., “Fuel Cell APU for Silent Watch and Mild Electrification of a Medium Tactical Truck.” *SAE Paper 2004-01-1477* (2004).

17. Lim, H., “Study of Exhaust Emissions from Idling Heavy Duty Diesel Trucks and Commercially Available Idle Reducing Devices.” *SAE Paper 2003-01-0288* (2003).

18. American Transportation Research Institute (Internet), *Compendium of Idling Regulations*, June 2008, (cited January 2009), http://atri-online.org/research/idling/atri_idlingcompendium7_11_08.pdf.

19. Kluger, M., Harris, J., “Fuel Economy Benefits of Electric and Hydraulic Off Engine Accessories.” *SAE Paper 2007-01-0268* (2007).

20. Page, R., Hnatczuk, W., Kozierowski, J., “Thermal Management for the 21st Century – Improved Thermal Control & Fuel Economy in an Army Medium Tactical Vehicle.” *SAE Paper 2005-01-2068* (2005).

21. Page, R., Bedogne, R., Steinmetz, T., “A “Mini-Hybrid” Transit Bus with Electrified Cooling System.” *SAE Paper 2006-01-3475* (2006).

22. Mancini, Bart. "Why Electric Accessories?." *HybriDrive® Propulsion System Cleaner, smarter power for transit*. Presented at Metro Transit, St. Paul, MN, 31 March 2009. BAE Systems.